
Biaxial mechanical evaluation of cholecyst-derived extracellular matrix: A weakly anisotropic potential tissue engineered biomaterial

James C. Coburn,^{1,2} Sarah Brody,^{1,2} Kristen L. Billiar,³ Abhay Pandit^{1,2}

¹National Centre for Biomedical Engineering Science, National University of Ireland, Galway, Ireland

²Department of Mechanical and Biomedical Engineering, National University of Ireland, Galway, Ireland

³Department of Biomedical Engineering, Worcester Polytechnic Institute, Worcester, MA

Received 27 February 2006; revised 13 May 2006; accepted 25 May 2006

Published online 31 January 2007 in Wiley InterScience (www.interscience.wiley.com). DOI: 10.1002/jbm.a.30943

Abstract: A new acellular, natural, biodegradable matrix has been discovered in the cholecyst-derived extracellular matrix (CEM). This matrix is rich in collagen and contains several other macromolecules useful in tissue remodeling. In this study, the principal material axes, collagen fiber orientations, and biaxial mechanical properties in a physiological loading regime were characterized. Fiber direction was determined by polarized light microscopy, and the principal axes and degree of anisotropy were determined mechanically. Macroscopic equibiaxial strain tests were then conducted on preconditioned specimens. While 13% of the area of CEM contains collagen fibers oriented between 50° and 60° from the neck-fundus axis, the principal material axis was oriented 63° ± 13.7°, with an aspect

ratio of 0.11 ± 0.06, indicating a weak anisotropy in that direction. Under biaxial loading, CEM exhibited a large toe region followed by an exponential rise in stress in both principal and perpendicular axis directions, similar to other materials currently under research. There was no significant difference between the biaxial stress-strain profile and the burst stress-strain profile. The results demonstrate that CEM is weakly anisotropic and it has the ability to support large strains across a physiological loading regime. © 2007 Wiley Periodicals, Inc. *J Biomed Mater Res* 81A: 250–256, 2007

Key words: extracellular matrix; biaxial; mechanical properties; principal axis; natural biomaterial

INTRODUCTION

One of the major goals in using natural biodegradable materials is to induce the host to replace the implanted construct with native tissue. Recently, xenographically-derived natural materials, typically of porcine origin, have been investigated for their apparent ability to elicit a regenerative response from host tissues rather than a normal healing response.^{1–4} These materials can be used for many different tissue engineering applications such as vascular grafts⁵ and repair of tendons,⁶ ligaments⁷ or body wall tissue.^{1,8} Increasing precision of design has led to batteries of tests to determine the properties of materials currently being used clinically and experimentally.^{8–11}

A new, natural material called cholecyst-derived extracellular matrix (CEM) has been developed in our

lab with potential applications in tissue engineering. Still in the preliminary stages, we are characterizing the biological and mechanical properties of the material to develop a practical implant more efficiently. CEM has been shown to allow complete ingrowth of cells as well as production of natural extra cellular matrix (ECM), when implanted subcutaneously.¹² Before developing the material for specific applications, we would like an improved understanding of its mechanical properties. Once the material properties are ascertained, CEM may be optimized for different applications.

The objective of the current study was to characterize the fibrous structure and the sub-failure and failure mechanical properties of CEM in several ways. First, the alignment of the fibrous structure was determined on both a microscopic and macroscopic level. Second, equibiaxial tensile tests were used to measure the material response along the principal directions. Finally, a burst test was done to characterize the failure strength of the material. An isometric material response was then derived from and compared to the biaxial results.

Correspondence to: A. Pandit; e-mail: abhay.pandit@nuigalway.ie

Contract grant sponsor: Enterprise Ireland, Technology Development Grant

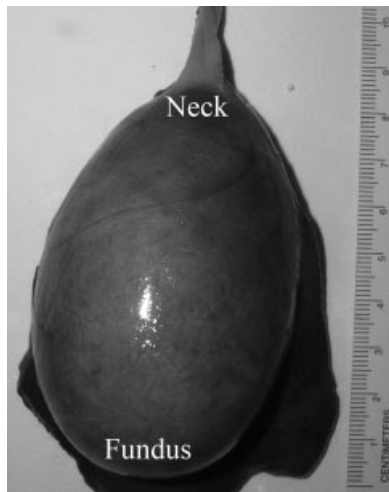


Figure 1. Gall bladder with the neck and fundus labeled. This direction was used as a basis for measurements of fiber orientation angle.

METHODS

Harvesting tissue samples

Cholecysts (gallbladders) were harvested from market weight pigs (Duffy Exports, Ireland) within 10 min of death and transported to the laboratory in a chilled icebox. CEM was isolated within 6 h of collection. First, the remnants of the liver were removed, and then the outer layer was cut off while the gall bladder was still full. After the outer layer was removed, the bile was drained from the gall bladder, and the neck and fundus regions (Fig. 1) were detached, so that the remaining tissue could be flattened out into a rectangular sheet. From that sheet, the inner mucosal layer was removed by mechanical delamination. The remaining CEM was then washed thoroughly in distilled water for at least five washes of 5 min each or until the water bath remained clear. The anatomical neck-fundus direction and outer side was noted and the material was cut into an asymmetrical shape to identify its side and orientation for subsequent experiments. Each sample for fiber orientation experiments was then stored separately in sterile distilled water until analyzed. Storage lasted no more than 2 days. The fiber orientations of two additional freeze dried, rehydrated samples were tested to ensure correspondence to mechanical tests. A separate group of samples were likewise cut, freeze-dried, and stored in a vacuum desiccator until rehydrated for mechanical testing. These samples were stored for no more than 1 week.

Principal material axis

The material principal axis of 11 samples was determined using a method derived from Choi and Vito.¹³ Briefly, the orientation of each sample was noted, and they were cut into circles measuring 44 mm. The samples were then affixed to a uniform elastic ring with hooks attached at 15° increments. The elastic ring had uniform elastic properties

and a low elastic modulus and did not interfere with the test. Its role was simply to aid in the accurate attachment of the hooks. Two hooks were attached to wires that loaded one direction with 0.98 N, while two hooks in the perpendicular direction were held at a constant separation of 44 mm, or zero displacement. Finally, two marks composed of permanent ink and high viscosity cyanoacrylate, approximately 1 mm in diameter, were made at a fixed distance of 40 mm along the stretched line of loading [Fig. 2(a)]. Each sample was then unloaded, rotated 15°, and reattached to the jig. The process was repeated for 180°. The ellipse formed by the dots was digitized, and the angle between the anatomical neck-fundus axis and the principal axis, on the mucosal side, was found [Fig. 2(b)]. An aspect ratio was calculated between the long and short radii of the ellipse. For this calculation, a ratio of zero denotes a circle with increasing eccentricity as the ratio increases.

Collagen fiber orientation

Asymmetrical samples of CEM ($n = 5$) were viewed using a polarized light microscope (PLM) with a birefringence imaging module (Metripol, Oxford Cryosystems, England), attached to the microscope (Prior Scientific, Cambridge, England). The polarization module, consisting of a series of specialized filters, an analyzer, and a rotating polarizer, was used to produce a ray of polarized light, which split into two mutually perpendicular vibrating rays as it passed through the birefringent CEM specimen. Retardance of one ray relative to that of the other was then measured by the microscope. For each area of CEM examined, 50 views were captured by a CCD camera at 3.6° intervals and merged to create a composite image of the area. The rotating polarizer facilitated this process. Composite images captured by the microscope consisted of three images: an orientation image depicting collagen orientation, a birefringence image demonstrating levels of birefringence of the area under investigation, and an intensity image representing light intensity. Data in these images was stored on a color map representing collagen fiber angle for the particular pixel. To calculate the preferred collagen fiber orientation, the number of pixels of a particular color in the orientation images was quantified

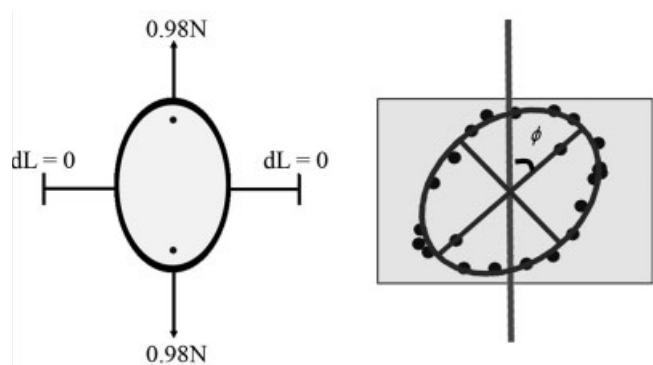


Figure 2. (a) Schematic representation of load and displacement boundary conditions. (b) Example of resulting marked ellipse and angle measurement.

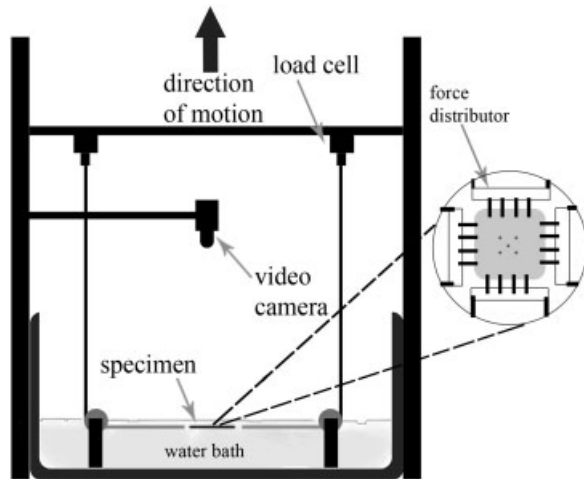


Figure 3. Schematic of biaxial testing machine with inset view of specimen labeled with optical markers.

using image analysis software (Image Pro[®], MD), and the percentage area of the sample under the microscope with fibers oriented at a particular angle was calculated. All samples were examined at 40 \times and 100 \times , but for image analysis and statistical analysis purposes, five composite images of each sample were captured at random locations at 100 \times and the orientation images were analyzed. In all cases, a filter that operates at a wavelength of 600 nm was used to polarize the light. Heart valves, whose collagen fiber orientation has previously been characterized, using the same method, were used as a control.¹⁴ Due to the semi-quantitative nature of the technique, results were represented in terms of percentage area covered with fibers in particular angle ranges. Angles were all measured relative to the neck-fundus axis on the mucosal side of the cholecyst and were binned in 10 $^\circ$ increments.

Biaxial test

Determination of the average principal axis allowed us to test the tissue specimens in a biaxial test. The testing machine consisted of a uniaxial load frame (Zwick Roell, Germany) fitted with custom tooling, comprising four load cells and four adjustable tension wires. These wires ran through a set of pulleys at the base of a temperature-controlled sample immersion tank. Tension could then be applied simultaneously in two horizontal directions at a constant equibiaxial strain rate (Fig. 3). A digital video camera was fitted above the specimen to record movement of high contrast dots. Both load frame and video data were collected concurrently.

Samples were cut into 2.5 cm squares with the edges ($n = 10$) parallel and perpendicular to the principal axis respectively. Four black ink dots, approximately 0.5 mm in diameter, were made in a ~ 5 mm square at the center using the same ink as the fiber orientation tests. Each side of the specimen was attached to the loading wire by four hooks through a load distributor (Fig. 3, inset).

Once loaded, samples were pre-tensioned to a reference state of 100 mN of force along each side. Specimens were

then strained at a rate of 5 mm/min up to a maximum strain of 50%, with a maximum allowed load of 5 N imposed to prevent premature sample failure. Green strain was calculated locally, using the ink marks, but controlled on a macro level because the machine was not capable of video feedback control. Six repetitions of each test were completed, and the data from the last test was used. It was determined that three to four preconditioning trials were necessary to obtain consistent results. All tests were carried out in a water bath of 0.9% saline at 37 $^\circ$ C.

Force and video extensometer data was synchronized and analyzed (MATLAB[®], Mathworks, MA). The stress-strain response curves were interpolated using a non-linear exponential best-fit curve to reduce noise. Stress was calculated using the Cauchy stress equations. As the stress-strain behavior was non-linear, the stiffness of the sample was defined as the Maximum Tangent Modulus (MTM), a measure of the modulus of the material in the high stress region.¹⁵

Burst test

An Instron hydraulic load frame (Instron Corp. MA) was fitted with a ball-burst jig, whose design was based on the *Standard Test Method for Bursting Strength of Knitted Goods, Constant-Rate-of-Traverse Ball-burst Test* (ASTM D D3787-01), and used to test seven freeze-dried, rehydrated samples of CEM. Briefly, each CEM sample was clamped in a 44.45 mm inner diameter ring with a roughened surface to prevent slippage. The specimens were then tested to failure by lowering a 25.4 mm steel ball through the specimen at a rate of 2 mm/s. The burst force was defined as the maximum force obtained before rupture of the specimen. The Instron was connected to a data acquisition system for recording the force and displacement of the cross-head throughout the running time of the experiment. Force displacement curves were smoothed with a fifth-order Gaussian function to remove load cell noise before further processing.

The ball-burst test directly determined the strength of the specimens, but a simple analytical model was used to determine more relevant material properties. In this technique, the model was solved piecewise for the spherical section "attached" to the ball and a conical section stretching between that and the clamp. The sections were divided along the radius where the sample left the sphere on a tangent for edge of the ring. The radius was found by the method of intersection of circles in 2-D.

The stress in the specimen under the ball was then found using the formula for uniform pressure in a spherical cap and the surface area of the tissue. For complete derivation, see Freytes, et al.¹⁶:

$$\sigma_s = \frac{F(\cos \phi + 1)}{2\pi t(2r \sin \phi + t)}$$

where the F is the force measured by the load cell, t is the thickness, r is the radius of the ball, and ϕ denotes the angle between the vertical axis and the line between the sphere center and the point of material detachment. MTM was then calculated from the stress-strain curves.

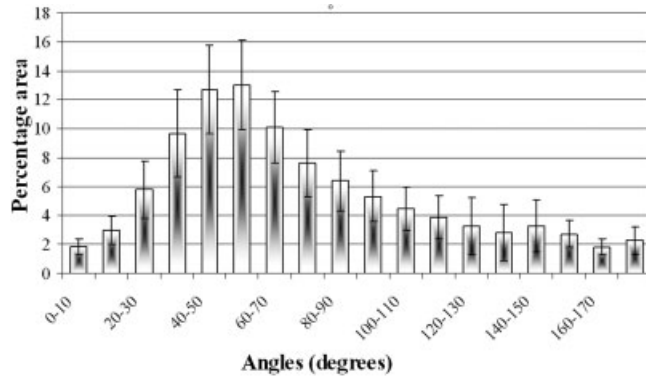


Figure 4. Orientation of collagen fibers in CEM as measured from the neck-fundus axis using PLM. Results show mean percentage (± 1 SD, $n = 5$).

Instant specimen thickness was calculated at each time interval, assuming incompressibility of the specimen, homogeneity of deformation across the specimen, and the observation that the tissue maintains the same basic shape. Initial specimen thickness was measured by placing the tissue between two glass slides and measuring the thickness with a micrometer, taking care not to compress the specimen.

Statistical analysis

Fiber orientations were compared to a theoretical isotropic sample using a Chi Square test. MTM results for both mechanical tests were compared using unpaired Student’s *t*-tests. Stress–strain results of the burst test at 1 MPa and the biaxial tests at 1 MPa were compared in the same way. A value of $p < 0.05$ was considered significant.

RESULTS

The fibrous meshwork of CEM is not completely isotropic. Measurements of the principal axis show that it lies at an angle of $63.7^\circ \pm 13.7^\circ$ to the anatomic neck-fundus axis. However, the material preference for this direction is relatively low with an elliptical aspect ratio of 0.11 ± 0.06 . CEM is a thin translucent material, thus providing high quality polarized light microscopy results. Thirteen percentage of the area of CEM is covered with collagen fibers oriented between 50° and 60° while only 1.8% of the area is covered with fibers oriented between 160° and 170° (Fig. 4). The preferred collagen fiber orientation was defined as the mode of the collagen fiber angles, identified as 55° . Fibers in this orientation were not, however, significantly more prevalent than in the isotropic case.

Equibiaxial strain tests were made along the principal and perpendicular axes. Three of the specimens contained recurrent artifacts due to external noise or showed signs of failure and were not included in the

final analysis. The seven CEM specimens analyzed exhibited typical hyperelastic properties (Table I). There was a large standard deviation in the MTM of the principal and perpendicular directions, yielding no significant difference between the two. Neither were significant differences found between the strain responses (Fig. 5). In agreement with the aspect ratio, the ratio of maximum strain shows that each sample does tend toward a less extensible principal axis.

Burst tests yielded similar curve trends to the biaxial results (Fig. 6). The average maximum values at burst are displayed in Table I. In the lower stress regime tested by the biaxial tester, the burst data shows no significant difference (Fig. 5). One sample failed prematurely due to imperfections and was removed from the sample data set. The MTM of the burst test analytical model was lower, but not statistically different from the biaxial tests with similar standard deviations. As in the biaxial tests, the preload reduced the overall strain to burst, but it was maintained for comparison with the biaxial results (Table I).

DISCUSSION

This preliminary assessment of the native properties of CEM establishes, through multiple measures, the material strength, degree of anisotropy, and basic stress–strain response. Other naturally-derived materials such as small intestinal submucosa (SIS)^{3–5,17} and urinary bladder matrix (UBM)^{18,19} have been tested extensively. CEM is a novel ECM derived from the porcine gallbladder, as yet uncharacterized. This primary characterization gives an insight as to possible applications such a material could support.

Previous studies on CEM have demonstrated that it has a low cellular and muscle content and high collagen content.²⁰ Collagen is an important load-bearing structural protein, and its structural configuration is therefore intrinsically related to CEM mechanical properties. The large standard deviation in principal

TABLE I
Average Mechanical Properties of CEM at Burst and During the Biaxial Tests

<i>Maximum biaxial test results</i>	
Principal MTSM (MPa)	38.29 \pm 11.90
Perpendicular MTSM (MPa)	36.51 \pm 10.99
Ratio of maximum strain	0.16 \pm 0.08
<i>Maximum burst test results</i>	
Displacement (mm)	14.90 \pm 1.97
Burst force (N)	30.26 \pm 8.37
Thickness (mm)	0.21 \pm 0.06
Max strain (%)	29.1 \pm 8.06
Max stress (MPa)	4.52 \pm 2.02
MSTM (MPa)	27.83 \pm 11.06

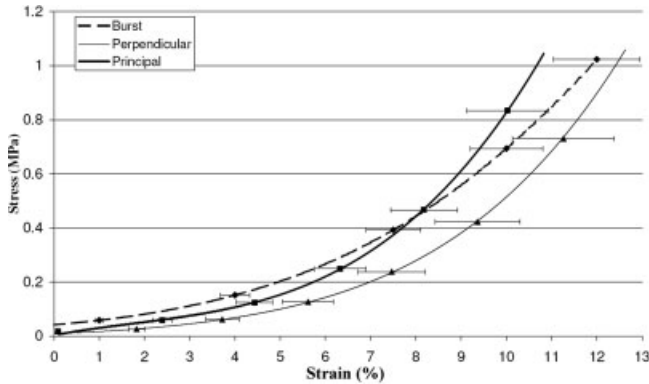


Figure 5. Stress and strain curves calculated under equibiaxial strain superimposed with the average data burst tests ($\pm 90\%$ confidence interval).

axis angle is a result of the low resolution of this technique and the low aspect ratio, or weak anisotropy, of the material. The accuracy of such a macroscopic technique is reduced, the closer a material is to isotropic. Allowing for the large standard deviation, these results agree with the PLM data showing actual fiber orientation.

Polarized light microscopy is a non-destructive technique, which does not necessitate the staining or labeling of tissue samples and has previously been used to identify collagen fiber structural configuration in other biological tissues including bone, cartilage and skin.^{21–23} Using a fixed polarizer, only sections of the crimped collagen fiber which were not aligned with the transmission axis of either polarizing filter would be visible under polarized light. This system used in this study incorporated circularly polarized light, which eliminated the dependency of brightness on sample orientation, and a rotating polarizer which facilitated the capture of 50 views of the same area at different angles, thereby allowing the complete visualization of the crimped collagen fibers.

Although a large proportion of the area of CEM consists of fibers oriented between 50° and 60° , studies on SIS identified a more distinct preferred collagen fiber orientation angle. The collagen fibers in SIS are oriented parallel to the long axis of the intestine with only occasional fiber populations oriented at approximately $\pm 28^\circ$.¹¹ Studies on bovine pericardium, an extensively studied biomaterial, have revealed a lesser degree of collagen fiber orientation and substantial inter and intra specimen variability,²⁴ similar to CEM. This difference between CEM, bovine pericardium and SIS may be due to the former's sac-like nature. The small intestine supports a system of active peristalsis whereas the pericardium and cholecyst are purely saclike structures. Without regular pressure and unidirectional flow, collagen fibers do

not have the mechanical stimuli that typically provoke alignment.²⁵

Biaxial test data confirmed that there were small differences between the stress–strain profile of the principal and perpendicular directions, but they were not statistically significant. Similar to other soft tissues,^{9,17,26} CEM exhibits a non-linear, hyperelastic material response. This biaxial test was run in equibiaxial strain, controlled by overall strain of the material. The calculated strains, which were taken from the video extensometry data, were not used in the control loop. This created discrepancies in the desired amount of strain imparted to each side of the tissue and the strain recorded by the extensometer. Video extensometer data was recorded from only the markers on the inner-most portion (25%) of the material, based on previous reports that edge effects are minimal in that region.²⁷ Square specimens were also used to reduce the asymmetrical strain effects induced by geometry.²⁸ The linear dimensions were taken along a line at the attachment points, which was slightly interior to the outer edge of the specimen. The principal fiber orientation of the material did not provide significantly greater stiffness than other directions.

The stress calculations for this model were validated by Freytes et al.¹⁶; however, they used a fifth order minimization to calculate the thickness of the material. By assuming that the tissue deforms uniformly and that there are no folds or wrinkles in the material during the test, we were able to calculate the thickness of the deformed shape, as if it were a disc of the same surface area as the deformed CEM. Because of this simplification, it was possible to calculate the entire stress–strain curve and determine its similarity to the biaxial data. These assumptions can lead to inaccuracies due stress concentrations or ma-

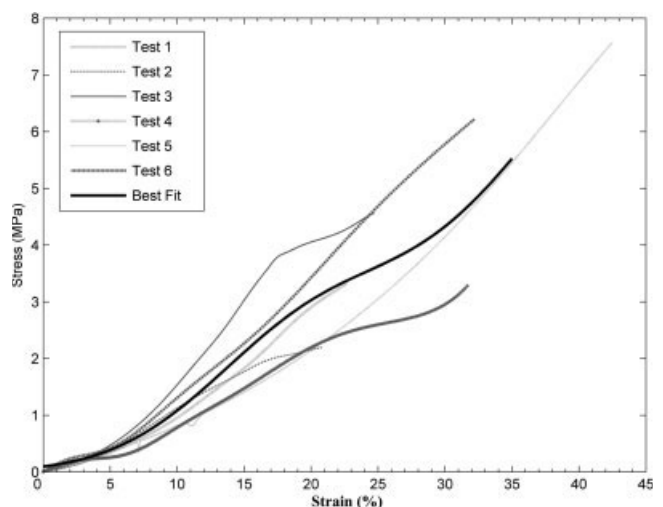


Figure 6. Stress and strain curves of the 6 burst tests (grey) and the best fit curve of all these tests (black).

terial imperfections that can alter the local deformation of the material. This may reduce the actually failure stress and strength of the material as well as change the local response to applied strain.

This idealized burst stress-strain model agrees well with the biaxial test data. The equi-biaxial data shows no significant difference in response between the principal and perpendicular directions. This implies that we can use the burst test to determine the strength of the material because it requires condition of planar symmetry. Because of the agreement burst stress and strain response below 1 MPa, it is a valid simplification of the biaxial test within this limited regime and can be used to simplify optimization experiments.

Comparisons between burst tests performed at different labs are difficult to make because they are dependent on the apparatus used. Typically, comparisons can only be made between samples tested with the same apparatus. Using stress and strain instead of absolute force and distension, we can extend the comparison to other burst apparatus. Natural materials have also proven to be strain rate invariant at low strain rates,²⁶ which increases the range of experiments that can be included in a comparison. Several other natural tissue-engineered materials have been tested using the same burst method. According to Freytes et al.¹⁹ four-layer SIS and two-layer UBM exhibit similar failure stresses to single layer CEM (5.69 and 3.54 respectively), but a two-layer UBM and urinary bladder submucosa composite exhibits a failure stress that is approximately twice that of CEM at 9.33 MPa. The MTM of all of these matrices was smaller than that of the CEM, indicating that overall, CEM is stiffer than those matrices. Though it has not been investigated in this study, CEM has the potential to be layered, increasing its strength as well. A naturally stiffer and stronger material such as CEM may increase the range of applications in which natural tissue engineered constructs are typically used.

It is important to note that the burst tests involved no preconditioning and therefore, capture the initial response of the material. Biological materials are shown to have hysteresis when loaded and must be preconditioned to the same loading regime in which they will be tested to obtain repeatable results. Practically, in most clinical applications, an implanted material will be subject to repeated strains and react as in the preconditioned case.²⁶

Optimizing the CEM to have the mechanical properties of a desired application can increase its biological desirability. To fully characterize each newly optimized material, it would be necessary to carry out a rigorous course of biaxial testing such has been done with other materials.^{9,17,29-31} According to the comparisons between the burst tests, biaxial data, and fiber orientation data, the burst test gives an accurate

approximation of the material's properties without the additional analysis of the more rigorous tests. The burst test can then be used to incrementally verify optimization of the CEM to a specific clinical application. Full characterization of the material may then be done only when the optimized properties are found.

CONCLUSIONS

CEM exhibits good strength and compliance in a physiologically relevant range of stresses and strains. The very weak anisotropic behavior of the material allows for greater freedom with design parameters than a strongly anisotropic behavior. The consistent, wider range of collagen fiber orientations increases the suitability of CEM as a material for multi-axial loading applications. With further development and optimization, this material could be tested in a range of clinical applications.

References

1. Badylak S, Kokini K, Tullius B, Simmons-Byrd A, Morff R. Morphologic study of small intestinal submucosa as a body wall repair device. *J Surg Res* 2002;103:190-202.
2. Franklin M, Gonzalez J, Glass J. Use of porcine small intestinal submucosa as a prosthetic device for laparoscopic repair of hernias in contaminated fields: 2-year follow-up. *Hernia* 2004;8:186-189.
3. Kropp BP, Cheng EY, Lin HK, Zhang Y. Reliable and reproducible bladder regeneration using unseeded distal small intestinal submucosa. *J Urol* 2004;172(4, Part 2):1710-1713.
4. Zhang Y, Kropp BP, Lin HK, Cowan R, Cheng EY. Bladder regeneration with cell-seeded small intestinal submucosa. *Tissue Eng* 2004;10(1/2):181-187.
5. Lantz GC, Badylak SF, Hiles MC, Coffey AC, Geddes LA, Kokini K, Sandusky GE, Morff RJ. Small intestinal submucosa as a vascular graft: A review. *J Invest Surg* 1993;6:297-310.
6. DeJardin LM, Arnoczky SP, Ewers BJ, Haut RC, Clarke RB. Tissue-engineered rotator cuff tendon using porcine small intestine submucosa: Histologic and mechanical evaluation in dogs. *Am J Sports Med* 2001;29:175-184.
7. Ledet EH, Carl AL, DiRisio DJ, Tymeson MP, Andersen LB, Sheehan CE, Kallakury B, Slivka M, Serhan H. A pilot study to evaluate the effectiveness of small intestinal submucosa used to repair spinal ligaments in the goat. *Spine J* 2002;2: 188-196.
8. Whitson BA, Cheng BC, Kokini K, Badylak SF, Patel U, Morff R, O'Keefe CR. Multilaminar resorbable biomedical device under biaxial loading. *J Biomed Mater Res* 1998;43:277-281.
9. Sacks MS, Chuong CJ. Orthotropic mechanical properties of chemically treated bovine pericardium. *Ann Biomed Eng* 1998;26:892-902.
10. Langdon SE, Chernecky R, Pereira CA, Abdulla D, Lee JM. Biaxial mechanical/structural effects of equibiaxial strain during crosslinking of bovine pericardial xenograft materials. *Biomaterials* 1999;20:137-153.
11. Sacks MS, Gloeckner DC. Quantification of the fiber architecture and biaxial mechanical behavior of porcine intestinal submucosa. *J Biomed Mater Res* 1999;46:1-10.

12. Burugapalli K, Chan J, Kelly J, Pandit A. Investigation of degradation and tissue response of cholecyst derived extracellular matrix. In the Proceedings of the Tissue Engineering Society International 2005; p 121.
13. Choi HS, Vito RP. Two-dimensional stress-strain relationship for canine pericardium. *J Biomech Eng* 1990;112:153–159.
14. Brody S, Anilkumar T, Lilensiek S, Last JA, Murphy CJ, Pandit A. Characterising nanoscale topography of the aortic heart valve basement membrane for tissue engineering scaffold design. *Tissue Eng*. Forthcoming.
15. Sacks MS, Chuong CJ. Characterization of collagen fiber architecture in the canine diaphragmatic central tendon. *J Biomech Eng* 1992;114:183–190.
16. Freytes DO, Rundell AE, Vande Geest J, Vorp DA, Webster TJ, Badylak SF. Analytically derived material properties of multilaminated extracellular matrix devices using the ballburst test. *Biomaterials* 2005;26:5518–5531.
17. Gloeckner DC, Sacks MS, Billiar KL, Bachrach N. Mechanical evaluation and design of a multilayered collagenous repair biomaterial. *J Biomed Mater Res* 2000;52:365–373.
18. Hodde JP, Record RD, Tullius RS, Badylak SF. Retention of endothelial cell adherence to porcine-derived extracellular matrix after disinfection and sterilization. *Tissue Eng* 2002;8:225–234.
19. Freytes DO, Badylak SF, Webster TJ, Geddes LA, Rundell AE. Biaxial strength of multilaminated extracellular matrix scaffolds. *Biomaterials* 2004;25:2353–2361.
20. Anilkumar T, Biggs M, Pandit A. Cholecyst-derived extracellular matrix: A potential scaffold. Presented at European Society for Biomaterials Conference, Sorrento, Italy, 2005.
21. Arokoski JP, Hyttinen MM, Lapvetelainen T, Takacs P, Kosztaczky B, Modis L, Kovanen V, Helminen H. Decreased birefringence of the superficial zone collagen network in the canine knee (stifle) articular cartilage after long distance running training, detected by quantitative polarised light microscopy. *Ann Rheum Dis* 1996;55:253–264.
22. Jacques SL, Roman JR, Lee K. Imaging superficial tissues with polarized light. *Lasers Surg Med* 2000;26:119–129.
23. Bigi A, Cacchioli A, Fichera AM, Gabbi C, Koch MH, Ragionieri L, Ripamonti A, Roveri N. X-ray diffraction and polarizing optical microscopy investigation of the structural organization of rabbit tibia. *J Biomed Mater Res* 1998;41:289–295.
24. Hiester ED, Sacks MS. Optimal bovine pericardial tissue selection sites. I. Fiber architecture and tissue thickness measurements. *J Biomed Mater Res* 1998;39:207–214.
25. Driessen NJ, Boerboom RA, Huyghe JM, Bouten CV, Baaijens FP. Computational analyses of mechanically induced collagen fiber remodeling in the aortic heart valve. *J Biomech Eng* 2003;125:549–557.
26. Lanir Y, Fung YC. Two-dimensional mechanical properties of rabbit skin. II. Experimental results. *J Biomech* 1974;7:171–182.
27. Billiar KL, Sacks MS. A method to quantify the fiber kinematics of planar tissues under biaxial stretch. *J Biomech* 1997;30:753–756.
28. Waldman SD, Lee JM. Effect of sample geometry on the apparent biaxial mechanical behaviour of planar connective tissues. *Biomaterials* 2005;26:7504–7513.
29. Lu SH, Sacks MS, Chung SY, Gloeckner DC, Pruchnic R, Huard J, de Groat WC, Chancellor MB. Biaxial mechanical properties of muscle-derived cell seeded small intestinal submucosa for bladder wall reconstitution. *Biomaterials* 2005;26:443–449.
30. Wells SM, Sacks MS. Effects of fixation pressure on the biaxial mechanical behavior of porcine bioprosthetic heart valves with long-term cyclic loading. *Biomaterials* 2002;23:2389–2399.
31. Billiar KL, Sacks MS. Biaxial mechanical properties of the native and glutaraldehyde-treated aortic valve cusp, Part 2: A structural constitutive model. *J Biomech Eng* 2000;122:327–335.